Redating the onset of the mid-Holocene sea-level highstand in southeast Australia and implications for global sea-level rise

Amy J. Dougherty[1], Zoë Thomas[2], Christopher Fogwill[2,3], Alan Hogg[4], Jonathan Palmer[2], Eleanor Rainsley[3], Alan N. Williams[2,5], Sean Ulm[6], Brian G. Jones[1], and Chris Turney[2],

[1]School of Earth and Environmental Science, University of Wollongong, Wollongong, 2522, Australia

[2]Palaeontology, Geobiology and Earth Archives Research Centre, and ARC Centre of Excellence for Australian Biodiversity and Heritage, School of Biological, Earth and Environmental Sciences, University of New South Wales, Australia

[3]School of Geography, Geology and the Environment, Keele University, ST5 5BG, UK

[4]Waikato Radiocarbon Laboratory, University of Waikato, Private Bag 3105, Hamilton, New Zealand

[5]Extent Heritage Pty Ltd, 3/73 Union Street, Pyrmont, NSW 2009

[6] ARC Centre of Excellence in Australian Biodiversity and Heritage, College of Arts, Society and Education, James Cook University, PO Box 6811, Cairns, QLD 4870, Australia

*Corresponding Authors

Email: adougher@uow.edu.au and c.turney@unsw.edu.au

Abstract

Reconstructing past sea levels can help constrain uncertainties surrounding the rate of change, magnitude, and impacts of the projected increase through the 21st century. Of significance is the mid-Holocene sea-level highstand in tectonically stable and remote (*far-field)* locations from major ice sheets. Considerable debate surrounds both the peak level and timing of the onset. The east coast of Australia provides an excellent arena in which to investigate changes in sea level during the Holocene. An east Australian site known as Bulli Beach provides the earliest evidence for the establishment of this highstand in the Southern Hemisphere, although questions have been raised about the pretreatment and type of material that was radiocarbon dated for the development of the regional sea level curve. Here we undertake a multidisciplinary study at Bulli Beach to constrain the onset of the Holocene highstand in eastern Australia. In contrast to wood and charcoal samples that may provide anomalously old ages, probably due to inbuilt age, we find that short-lived terrestrial plant macrofossils provide a robust chronological framework. Bayesian modelling of the ages provides the most precise dating of the highstand which was established at 6,880±50 calendar years ago. Our results are consistent with a growing body of evidence extending from the Gulf of Carpentaria to Tasmania that suggest a synchronous onset, independent of isostatic changes across eastern Australia, and coherent with major ice mass loss from Antarctica. Further work is now needed to refine the structure of the sea-level highstand, the timing of the sea-level fall in the late-Holocene and their impacts on coastal evolution.

Introduction

Whilst global sea level has risen through the twentieth century and is expected to increase into the future, considerable uncertainties surround the timing, magnitude and impact of projected change (1, 2). A major cause of this uncertainty is the short nature of the historic record and the limited range of observed changes compared to the recent geological past (3, 4), especially the response of ice sheets to warming (5-10). The situation is exacerbated during the last century with sea-level rise being dominated by thermosteric effects (11). Although the historic record can be extended back millennia by exploiting natural archives sensitive to sea-level change, including coastal sedimentary and geomorphological features (12-15), there is an urgent need for a greater network of sites in time and space (16). This is particularly so given the non-linear nature of coastal inundation as a result of sea-level rise (17-19) and the major associated environmental and socio-economic impacts projected for the 21st century (20-22).

Since the Last Glacial Maximum (LGM) at c. 21,000 years ago (23), sea level has risen some 120 m to present mean sea level (PMSL) (24). However, this rise in sea level has not been uniform but punctuated by abrupt increases (and some decreases) with other periods of limited change (25-29). Globally, these changes had far-reaching impacts on both humans and ecosystems, particularly in Australia, which has an extensive network of archaeological and environmental records spanning the last 50,000 years (30-33). Importantly, the spatial and temporal changes that occurred through the Holocene (the last 11,650 years) remain unclear (28, 34-36). Potentially important is the mid-Holocene sea-level highstand which may provide an analogue for the future and has been reported across Australasia and the wider Southern Hemisphere (37-40). Critically, although the onset of this period approximately spans 8,000 to 7,000 years ago, reconstructions of changing sea-levels (using a variety of intertidal deposits including estuarine deposits and sub-fossil mangroves; (41, 42) suggest significant spatial and temporal variability (38).

The origin of this early sea-level highstand remains unclear. Recent work has suggested that prolonged meltwater flux sustained the highstand through much of the Holocene (38, 43). The establishment of the Australia Holocene sea-level highstand at 8,000 years ago is surprising given the remote (*far-field*) location from major ice sheets (34). Global ice sheets lost considerable mass after the LGM (23), with significant mid-Holocene ice-mass loss reported from the West and East Antarctic Ice Sheets (e.g. 44, 45), and ongoing mass loss from Greenland throughout the Holocene (e.g. 46, 47). If ice mass loss was a cause of the persistent sea-level highstand, the East and West Antarctic Ice Sheets are reported to have experienced dramatic drawdown around 7,000 years ago (10, 44), approximately a millennium before the highstand reported from Australia. Given the recently reported loss of Antarctic ice mass (5) and the sensitivity of ice sheets to greenhouse gas forcing (9, 48), the relationship to regional sea-level highstands needs to be better constrained.

Far-field sites that are tectonically quiescent, such as Australia, are of global significance as they are most likely to preserve the purest record of ice-equivalent eustatic sea level (34). Because of glacio-eustatic changes following the LGM, modelling studies suggest the eastern Australian coast has responded slowly to the reduction in global ice volume, and that sea-level reached its present level between 9,000 and 7,000 years ago (49), on which tectonic influences are superimposed (35). Despite extensive study, reconstructions from the Australian coast have struggled to reconcile the debate regarding the timing and elevation of a mid-Holocene sea-level highstand (38). For instance, in northeast Australia (Queensland) it is currently accepted that a highstand of 1 to 1.5 m above PMSL was reached around 7,000 years ago (35). Conversely, in southeast Australia, early research suggested that sea-level reached present-day elevations 7,000 years ago and maintained PMSL through the mid- to late- Holocene (41, 50). Subsequent work, from a site ~80 km south of Sydney called Bulli Beach, however, has provided evidence for an early Holocene sea-level highstand of +1.84 m possibly dating back as early as 8,000 years ago (42, 51, 52). The elevation and timing currently reported from Bulli Beach is anomalous, however, not just within Australia (38), but globally (34). Importantly, virtually all of the data informing on this early Holocene highstand from Australia are from Bulli Beach and proximal sites (38).

Here we report on a detailed study revisiting the elevated estuarine sediments at Bulli Beach to better constrain the onset and magnitude of the Holocene sea-level highstand and place these results in a global context.

Previous studies

Bulli Beach, also known as Sandon Point Beach (hereafter ‘Bulli’) is approximately 900 m long with a varying width due to storm cut-and-fill (Fig 1). The modal beach state for Bulli grades between ‘Transverse Bar’ and ‘Rip to Low Tide Terrace’ and average wave heights range from 0.5 m in the south to 1 m in the north (53). Bulli Beach is the seaward portion of a receded barrier complex that is covered with fill. The receded nature of this system is demonstrated by periodic erosion exposing an outcrop of grey, sandy estuarine mud in front of the barrier/fill and along the banks of an inlet called Slacky Creek. Typically following an erosive event, a post-storm recovery bar/ridge impounds Slacky Creek causing it to run parallel to shore and ultimately reburies the deposit (Fig 1c and d).

A series of storms in the 1970s culminated in severe erosion at Bulli in 1978, exposing extensive early to mid-Holocene sedimentary deposits centered on Slacky Creek. Jones *et al.,* 1979 (51) performed a comprehensive study of the Bulli barrier system using detailed coring and field mapping that capitalized on an extensive exposure of the usually buried back-barrier muds (Fig 2a) and identified four Quaternary units. The basal unit consists of Pleistocene fluvial muddy sands overlain by mottled estuarine mud sediments. The upper Holocene deposits are a grey, sandy estuarine mud capped by an upper sand unit representing the receded barrier that has been covered with fill to an elevation of 4 m above PMSL. Radiocarbon dating of wood, charcoal and shell material exposed within the estuarine mud at elevations between PMSL and +1.49 m appeared to suggest sea level has reached its present position between 7,500 and 6,400 BP (51). This pioneering work also recognized a grey sandy mud unit at Thirroul (just north of Bulli) where ages obtained from charcoal (8,300±150 BP, equivalent to 9,210±190 cal BP) and a Myrtaceae root (7,000±150 BP, equivalent to 7,800±140 cal BP) were located 1.84 m above PMSL, although their provenance and association with Bulli was considered uncertain (51). Note that the radiocarbon ages calibrated here used SHCal13 (54) and henceforth all calibrated radiocarbon ages are expressed as cal BP while uncalibrated ages are designated as BP. More than a decade after the benchmark study by Jones *et al.,* 1979 (51), Bryant *et al.,* 1992 (52) returned to Bulli and Thirroul as well as a neighboring site called MacCauleys Beach. Radiocarbon (^{14}C) dating of shell and *in situ* mangrove stumps from estuarine deposits and thermoluminescence dating of quartz sand from beach deposits at elevations of 1-2 m above PMSL gave ages ranging between 6,900 BP and 1,520 BP respectively. The timing of this mid-Holocene elevation highstand agrees with other results determined along the east coast of Australia and other far-field sites across the Southern Hemisphere (34, 38).

The above datasets have been utilized and combined with other records to construct regional sea level curves for southeast Australia (38, 42). Notably, the ages reported by Jones *et al.*, 1979 (51) and Bryant *et al.*, 1992 (52) form all the early data points above PMSL (>7,000 years ago), marking the onset of mid-Holocene highstand, approximately a millennium prior to that elsewhere (34, 42). While these more recent studies have recalibrated the older ages, and provided vertical error uncertainties to the sea-level reconstruction, these sites have not been revisited or had new data collected.

Methods

Here we report an extensive multidisciplinary study of this important area over several years. Initially Ground Penetrating Radar (GPR) was used to image the shallow subsurface and map the lateral extent of the deposit exposed during the 1978 storm, which was subsequently buried by modern beach and dune processes. Augers used to ground-truth the GPR did not penetrate the estuarine mud. Over the following three years the Bulli Beach site was monitored for exposure of back-barrier sediments. Finally, coring through the modern beach and dune sands was undertaken to sample these deposits in 2016. Shortly after coring, a major storm in June of that year re-exposed the deposits allowing surface and outcrop sampling.

Ground penetrating radar

GPR transects were collected perpendicular to the shoreline at Bulli in the central portion of the barrier (Fig 2). The GPR was collected in a grid configuration in order to produce a 3D image of the buried estuarine surface (55). The GPR transects and associated beach profiles were topographically surveyed using a Dumpy Level. A SIR-3000 digital GPR system with a

200 MHz antenna from GSSI (Geophysical Survey System Inc., USA) was used to acquire the geophysical records. Processing (topographic corrections, normalization, stacking and depth conversions) and analyses were performed on unfiltered data using RADAN7 Software and 3D Module. Unfiltered data were used in the analysis, because GPR records are subject to noise at a range of frequencies, and only modest improvements were attained in radar stratigraphy following the use of a Finite Impulse Response filter, as well as filtering of phantom hyperbola and minor antenna ringing (39). Gain adjustments were made in both processing and presentation of some records to increase the signal amplitude and the display resolution of stratigraphy. Travel-time was converted to depth in RADAN based on estimated dielectric constants (56) and ground-truthed using a hand auger. Sediments recovered from the auger were analyzed using standard sedimentological techniques for grain-size, sorting, rounding, and composition for comparison to the geophysical record of barrier facies. The interpretations of the recorded facies are described following the terminology of van Heteren *et al.*, 1998 (56) and facies interpretations are guided by Jones *et al.*, 1979 (51).

Sampling

On the south side of Slacky Creek at Bulli Beach (34.335˚S, 150.925˚E) coring of the estuarine sedimentary deposit below the upper sand unit defined by Jones *et al.,* 1979 (51) was undertaken using a modified 5-cm diameter Livingstone corer. The corer was drilled through the estuarine sediments down to a level of -0.15 m PMSL. We were not able to penetrate the base of the estuarine sediments. The exposed section was surveyed using a dumpy level across the site, with altitudes relative to PMSL/AHD (Australian Height Datum, the official height datum for the country and equates to mean sea level). This was grounded to a survey datum based on the bridge immediately inland of the site (as used by Jones *et al.* 1979), which was resurveyed for this study using differential GPS. Following the storm of

June 2016, extensive deposits of estuarine sediments were exposed on both sides of Slacky Creek. On the north side (34.334˚S, 150.925˚E) large wood fragments, including a *Melaleuca* log, were identified in the upper part of the deposit (Fig 3). Surface samples of wood were collected from the exposure (including two contiguous blocks of wood from the outer part of the *Melaleuca* log) for ^{14}C dating. No surface deposit with an elevation of +1.49 m was identified (Fig 3c) (51). During repeated visits north of Bulli Beach to Thirroul (2.5 km north of Bulli), we were unable to locate the exposure from which the highest point of the Holocene highstand had been reported (51). However, following the June 2016 storm, exposures of sloping mottled estuarine sediments were exposed 1.2 km north of Bulli at 0.6 m PMSL, McCauley's Beach (34.324˚S, 150.925˚E) (52). Surface samples of degraded wood were collected for ^{14}C dating.

Radiocarbon dating and age modelling

To collect a series of stratigraphically-constrained ages from Bulli Beach, the cores from the south side of Slacky Creek were extracted in the laboratory and subsamples were selected, soaked in Milli-Q™ grade water and sieved through a 100 micron sieve. Short-lived terrestrial plant macrofossils, comprising fruits and leaves, formed the focus of our study, being fragile and less likely to be integrated intact into the sediments if remobilized (57). Here we assume the contemporary sea level at the time these samples were deposited on the surface of estuarine floor may have been up to 0.5 m lower than the measured height (42). For ^{14}C dating, these samples were given an acid-base-acid (ABA) pretreatment, comprising 1N HCl at 70°C, rinsed and treated with multiple hot (70˚C) 1N NaOH washes. The NaOH insoluble fraction was treated with 1N HCl at 70°C, filtered, rinsed and dried. Because some of the oldest ages previously reported for the highstand were reported from bulk wood (e.g. an *in situ* stump from +1.09 m of 6890±220 BP reported by Bryant *et al*., 1992), we undertook alpha-cellulose extraction of this material type. Chemical pre-treatment of the wood samples resulted in the purification of alpha-cellulose as this wood fraction is deemed the most reliable for minimizing potential contamination and providing the most robust ^{14}C ages required for such high-precision study (58). Alpha-cellulose extraction begins with an ABA pretreatment at 80°C, with samples treated with 1N HCl for 60 min, followed by successive 30 min treatments with 1N NaOH until the supernatant liquid remained clear, ending with another 60 min 1N HCl wash. Holocellulose was then extracted by using successive 30 min treatments of acidified $NaClO_2$ at 70°C until the wood shavings were bleached to a pale-yellow color. Alpha-cellulose was then prepared by a final treatment with NaOH followed by a further acid wash (1N HCl at 70°C for 30 min), and repeated washing with distilled water until a pH of >6 was achieved. Samples were combusted and graphitized in the Waikato Radiocarbon Laboratory and $^{14}C/^{12}C$ measured by Accelerator Mass Spectrometry (AMS) at the University of California at Irvine (UCI).

The ^{14}C ages were used to develop an age model using a P_sequence deposition model in OxCal 4.2 (59, 60) with the General Outlier analysis detection method (probability=0.05) (61). The ^{14}C ages were calibrated against the Southern Hemisphere calibration (SHCal13) dataset (54). The model was based on 1,000 iterations. Using Bayes' theorem, the algorithms employed sample possible solutions with a probability that is the product of the prior and likelihood probabilities (59). Taking into account the deposition model and the actual age measurements, the posterior probability densities quantify the most likely age distributions; the outlier option was used to detect ages that fall outside the calibration model for each group, and if necessary, down-weight their contribution to the final age estimates (Table 1 and Fig 4).

Results and Discussion

Evidence for a sea-level highstand at Bulli

The GPR data collected at Bulli clearly imaged the estuarine muds from Jones e*t al.*, 1979 (51) (Fig 2b and c). The top of this facies is well defined by a strong, flat to stepped reflection that is laterally extensive at ~1 m above PMSL (Fig 2b-e) similar to that exposed in the 1978 storm (Fig 2a). The overlying beach facies consists of medium strength seaward and landward dipping reflections between ~1-2 m above sea level, imaging beach and berm stratigraphy. Within the landward berm stratigraphy, a ridge and runnel feature exists that captures a post-storm berm that migrated onshore, pinning Slacky Creek along the barrier until the channel becomes filled with beach and dune sands (best seen in Fig 2c). Hand augers indicate beach sediments are comprised mainly of medium to coarse grained quartz sand. The overlying dune sands are expressed in the thin uppermost facies in the central portion of the GPR and display a reflection-free signal to a depth of ~2 m above PMSL (Fig 2b-d). This homogenous geophysical signature is representative of the well-sorted, fine-grained, quartz-rich sand, transported by aeolian processes. Where the berm is wider in the south, incipient dune vegetation has colonized the relatively flat-lying aeolian veneer (Fig 2c).

Within the attenuated signal beneath the fill there is a layer preserved above the estuarine mud that was not imaged in the GPR but was recorded by outcrop mapping (Fig 3). The base of this facies on the south side of Slacky Creek between 1.26-1.28 m above PMSL comprises a coarse-grained limonite layer described as the base of the upper sand unit recognized by Jones *et al.*, 1979 (51). Importantly, limonite represents a mixture of similar hydrated iron oxide minerals, formed as a result of oxidation in water-rich sediment (62), and commonly found within marshy sediments (63). The presence of limonite is consistent with the establishment of floodplain sediments at elevated sea-level (Fig 3).

Dating the onset of the Holocene sea-level highstand

Previous work on the Holocene highstand at Bulli and the wider area has highlighted the offset between ages obtained from different materials (for example, wood and charcoal) and components (cellulose and bulk) (51, 52). These differences have been widely reported from other contexts (e.g. 64, 65, 66), raising the possibility that the early highstand of ~8 ka cal BP (34, 38) may be related to pretreatment and/or reworking of older material, rather than reflecting a true event. To investigate these issues, we undertook a comprehensive dating program of wood, charcoal and short-lived plant macrofossils (Table 1).

The short-lived terrestrial plant macrofossils provide a robust sequence of ages from the south side of Slacky Creek indicating accumulation began at 6,610±20 BP (-0.15 m PMSL; Wk-43689) to 6,100±20 BP (+1.19 m PMSL; Wk-43685) (Table 1). Bayesian age modelling of the series suggests the sediments represent a period spanning 7,450±30 cal BP to 6,880±50 cal BP (Fig 4). In contrast, a charcoal sample taken immediately underlying the limonite layer and representing the highest point of the estuarine sediments in our sequence (+1.26 m PMSL), reported a radiocarbon date of 6,720±20 BP (Wk-43684), significantly older than the ages obtained from the short-lived macrofossils dated below it (Fig 4). Unfortunately, no terrestrial macrofossils were identified in this uppermost sample. Importantly, radiocarbon dated surface wood on the north side of Slacky Creek at comparable heights to the uppermost sediments on the south side (+1.27 m PMSL), reported similarly older ages of 6,530±20 BP (Wk-43819) and 6380±20 BP (Wk-43820) (Table 1). Similarly, at a relatively lower elevation, the ages obtained from McCauley’s Beach at +0.6 m PMSL were also relatively older compared to the Bulli Beach (south Slacky Creek series), with the oldest age obtained being 6,820±20 BP (Wk-43923).

Our results are consistent with reworking and subsequent re-incorporation of wood and charcoal into the estuarine sediments, suggesting these are not reliable material types for dating the timing of sea-level change (at least at Bulli and the immediate area). Inbuilt ages due to wood and charcoal deriving from the older inner parts of trees may also contribute to the discrepancies observed. More importantly, however, is that Bayesian age modelling helps refine the timing and rate of sea-level rise in the approach to the highstand. In contrast to other studies investigating datasets comprising individual dated site locations (e.g. 38, 42), Bayesian age modelling is able to exploit a stratigraphically-constrained sequence of ages (60, 61), providing additional chronological control. Whilst we find the rate of sea-level rise is consistent with previous studies (38, 42), our findings indicate that the highstand represented by the remaining sediments at Bulli was reached around 6,880±50 cal BP, approximately one millennium later than previously reported elsewhere (34, 44) (Fig 5).

Wider Implications

The refined age modelling of short-lived plant macrofossils provides a coherent rise in sea level from PMSL at 7,500 cal BP to a high sea-level stand of +1.19 m at 6,900 cal BP (Fig 5). Our Bayesian age modelled suite of radiocarbon ages provide a coherent chronological framework for Bulli Beach (southeast Australia) and suggest the onset of the mid-Holocene sea-level highstand occurred approximately a millennium later than previously reported (42). Importantly, our new results agree with other records from the Sydney region. Roy and Crawford, 1976 (67) obtained a comparatively young ^{14}C age from Kurnell Peninsula at PMSL of 6,220±115 BP (7,070±140 cal. years BP) from a fossil mangrove stump (*Avicennia* *marina*), which in contrast to the original interpretation, more likely reflects an early part of the Holocene rise and not a stabilization of sea-level (Figs. 1 and 5). An oyster shell from Minnamurra, ~40 km south of Bulli (42) (Fig 1) recorded an age of 5,950±120 BP (6,380±150 years cal BP; calculated using Marine13 and a ΔR value of 3±69 (68, 69)) at +1 m PMSL is also consistent with our findings (Fig 5).

We therefore conclude that irrespective of the pretreatment method used, the relatively old reported ages from Bulli and surrounding environments that have been used to generate a regional sea-level curve appear to be the product of reworked material (Fig 5). Crucially, our results suggest a coherent picture of synchronous elevated high sea-level along the east coast of Australia (38) extending from the Gulf of Carpentaria to Tasmania (14, 37, 70), with no obvious major discrepancies in timing. Taken together our results support the onset of a continental-wide sea-level highstand shortly after 7,000 cal BP.

The timing of the onset of the Holocene highstand was a critical period in the formation and development of hunter-gatherer societies, which were likely only just recovering from displacement and adjustments stemming from the rapid inundation of the continental shelf during the terminal Pleistocene (36, 70, 71). Ongoing sea-level rise to the Holocene highstand would have impacted productive coastal environments, and further reduced the spatial area within which populations could move and occupy. This would likely have required ongoing changes in mobility, technology and behavior. Previous studies have assigned numerous Holocene technological and behavioral changes (e.g. diversification of archaeological sites, microlithisation of stone artefacts, expansion of *Pama-Nyungan* language, and proliferation of Panaramitee rock art style) to ameliorating climate (31). These changes instead may partly reflect increased packing of populations along the likely well utilized eastern seaboard. These areas still contain some of the densest populations of the continent. Archaeologically, it is important to highlight that the highstand would have resulted in the modification and/or loss of any coastal sites that would have formed between the terminal Pleistocene (Meltwater Pulse 1a) and ~6,900 cal years BP and as such, researchers focusing on this time period need to carefully consider their interpretations for taphonomic bias.

Importantly, the revised ages from eastern Australia are consistent with global studies (34). Furthermore, our results align with the timing of major mass loss from the West and East Antarctic Ice Sheets (44, 45). Arguably the best dated sequence from the East Antarctic is the Mount Suess/Gondola Ridge that lies adjacent to the main flow path of Mackay Glacier (Victoria Land; Fig 1), and which records substantial ice-sheet lowering by 6800 cal BP, comparable with the redefined onset of the Holocene highstand at Bulli Beach (Fig 5) (44). Previous work has suggested that ice-sheet mass loss sustained the elevated sea-level along the east coast of Australia (38, 43). Our results support this proposal. Future work is needed to more precisely constrain the timing and impact of Holocene ice mass loss and regional/global sea-level rise.

Conclusions

Reconstructing past sea level can help constrain uncertainties surrounding the rate of change, magnitude and impacts of projected increases through the 21st century. Of significance is the mid-Holocene sea-level highstand (+1 m PMSL) which potentially provides an analogue for 21st century warming. In Australia, considerable debate surrounds its existence and timing of onset, which has hitherto been considered spatially and temporally complex. Crucially a single area known as Bulli Beach in southeast Australia provides the earliest evidence for the establishment of this highstand in the Southern Hemisphere. However, the initial studies have been critiqued, notably in relation to sample pretreatment and material type.

Here, we revisit Bulli Beach and undertake a multidisciplinary study, identifying the deposits using GPR, field surveying, and a comprehensive dating program. We find that regardless of the pretreatment method used, wood and charcoal samples provide anomalously old ages, probably the result of in-built age. Instead, we targeted short-lived terrestrial plant macrofossils that more accurately reflects the timing of any sea-level change. Bayesian age modelling of stratigraphically-constrained series of ages from these types of samples provides a method for reducing the envelope of uncertainty of sea-level rise, and suggests the onset of the mid-Holocene highstand was established 6,880±50 cal BP. This is consistent with other records from across Australia and globally. Further work will refine the structure of the sea-level highstand and the timing of the sea-level fall in the late Holocene.

Acknowledgements

This work was supported by Australian Research Council (FL100100195 and CE170100015). We thank Professor Christopher Bronk Ramsey at Oxford University for his advice with OxCal modelling and John Southon from the University of California for measuring the $^{14}C/^{12}C$ ratios. SU is the recipient of an Australian Research Council Future Fellowship (project number FT120100656). Special thanks to Robert and Ann Young for the guided tour of the site and photos taken of it after the 1978 storm (one featured in Fig2a).

References

1. Horton BP, Rahmstorf S, Engelhart SE, Kemp AC. Expert assessment of sea-level rise by AD 2100 and AD 2300. Quaternary Science Reviews. 2014;84:1-6.

2. Church JA, Clark PU, Cazenave A, Gregory JM, Jevrejeva S, Levermann A, et al. Sea Level Change. In: Stocker TF, Qin D, Plattner G-K, Tignor M, Allen SK, Boschung J, et al., editors. Climate Change 2013: The Physical Science Basis Contribution of Working Group I to the Fifth Assessment Report of the Intergovernmental Panel on Climate Change. Cambridge, United Kingdom and New York, NY, USA: Cambridge University Press; 2013.

3. Slangen ABA, Church JA, Agosta C, Fettweis X, Marzeion B, Richter K. Anthropogenic forcing dominates global mean sea-level rise since 1970. Nature Climate Change. 2016;6:701.

4. Grinsted A, Moore JC, Jevrejeva S. Reconstructing sea level from paleo and projected temperatures 200 to 2100 ad. Climate Dynamics. 2010;34(4):461-72.

5. Shepherd A, Ivins E, Rignot E, Smith B, van den Broeke M, Velicogna I, et al. Mass balance of the Antarctic Ice Sheet from 1992 to 2017. Nature. 2018;556:pages219–22.

6. Shepherd A, Fricker HA, Farrell SL. Trends and connections across the Antarctic cryosphere. Nature. 2018;558(7709):223-32.

7. DeConto RM, Pollard D. Contribution of Antarctica to past and future sea-level rise. Nature. 2016;531:591.

8. Hay CC, Morrow E, Kopp RE, Mitrovica JX. Probabilistic reanalysis of twentieth-century sea-level rise. Nature. 2015;517:481.

9. Golledge NR, Kowalewski DE, Naish TR, Levy RH, Fogwill CJ, Gasson EGW. The multi-millennial Antarctic commitment to future sea-level rise. Nature. 2015;526:421.

10. Fogwill CJ, Turney CS, Meissner KJ, Golledge NR, Spence P, Roberts JL, et al. Testing the sensitivity of the East Antarctic Ice Sheet to Southern Ocean dynamics: past changes and future implications. Journal of Quaternary Science. 2014;29(1):91-8.

11. Fischer H, Meissner KJ, Mix AC, Abram NJ, Austermann J, Brovkin V, et al. Palaeoclimate constraints on the impact of 2 °C anthropogenic warming and beyond. Nature geoscience. 2018;11:474-85.

12. Buynevich IV, Fitzgerald DM, Smith Jr LB, Dougherty AJ. Stratigraphic evidence for historical position of the East Cambridge shoreline, Boston Harbor, Massachusetts. Journal of Coastal Research. 2001;17(3):620-4.

13. Massey AC, Gehrels WR, Charman DJ, White SV. An intertidal foraminifera-based transfer function for reconstructing Holocene sea-level change in southwest England. The Journal of Foraminiferal Research. 2006;36(3):215-32.

14. Dougherty AJ. Punctuated transgression (?): Comment on Oliver, T.S.N., Donaldson, P., Sharples, C., Roach, M., and Woodroffe, C.D. "Punctuated progradation of the Seven Mile Beach Holocene barrier system, southeastern Tasmania". Marine Geology. In Press.

15. Hein CJ, FitzGerald DM, Thadeu de Menezes J, Cleary WJ, Klein AHF, Albernaz MB. Coastal response to late-stage transgression and sea-level highstand. Geological Society of America Bulletin. 2014;126(3-4):459-80.

16. Dutton A, Carlson A, Long A, Milne G, Clark P, DeConto R, et al. Sea-level rise due to polar ice-sheet mass loss during past warm periods. Science. 2015;349(6244):4019.

17. Sweet WV, Park J. From the extreme to the mean: Acceleration and tipping points of coastal inundation from sea level rise. Earth's Future. 2014;2(12):579-600.

18. Thomas ZA. Using natural archives to detect climate and environmental tipping points in the Earth System. Quaternary Science Reviews. 2016;152:60-71.

19. Lenton TM, Held H, Kriegler E, Hall JW, Lucht W, Rahmstorf S, et al. Tipping elements in the Earth's climate system. Proceedings of the National Academy of Sciences. 2008;105(6):1786-93.

20. Neumann B, Vafeidis AT, Zimmermann J, Nicholls RJ. Future coastal population growth and exposure to sea-level rise and coastal flooding-a global assessment. PloS one. 2015;10(3):e0118571.

21. Bellard C, Leclerc C, Courchamp F. Impact of sea level rise on the 10 insular biodiversity hotspots. Global Ecology and Biogeography. 2014;23(2):203-12.

22. Nicholls RJ, Wong PP, Burkett VR, Codignotto JO, Hay JE, McLean RF, et al. Coastal systems and low-lying areas. In: Parry ML, Canziani OF, Palutikof JP, van der Linden PJ, Hanson CE, editors. Climate Change (2007): Impacts, Adaptation and Vulnerability Contribution of Working Group II to the Fourth Assessment Report of the Intergovernmental Panel on Climate Change. Cambridge, UK Cambridge University Press; 2007. p. 315-56.

23. Clark PU, Dyke AS, Shakun JD, Carlson AE, Clark J, Wohlfarth B, et al. The last glacial maximum. science. 2009;325(5941):710-4.

24. Ishiwa T, Yokoyama Y, Miyairi Y, Obrochta S, Sasaki T, Kitamura A, et al. Reappraisal of sea-level lowstand during the Last Glacial Maximum observed in the Bonaparte Gulf sediments, northwestern Australia. Quaternary International. 2016;397:373-9.

25. Leonard ND, Welsh KJ, Clark TR, Feng Yx, Pandolfi JM, Zhao Jx. New evidence for “far-field” Holocene sea level oscillations and links to global climate records. Earth and Planetary Science Letters. 2018;487:67-73.

26. Lewis SE, Wüst RAJ, Webster JM, Collins J, Wright SA, Jacobsen G. Rapid relative sea-level fall along north-eastern Australia between 1200 and 800cal.yrBP: An appraisal of the oyster evidence. Marine Geology. 2015;370:20-30.

27. Turney CSM, Brown H. Catastrophic early Holocene sea level rise, human migration and the Neolithic transition in Europe. Quaternary Science Reviews. 2007;26(17):2036-41.

28. Lambeck K, Chappell J. Sea Level Change Through the Last Glacial Cycle. Science. 2001;292(5517):679-86.

29. Hanebuth T, Stattegger K, Grootes PM. Rapid Flooding of the Sunda Shelf: A Late-Glacial Sea-Level Record. Science. 2000;288(5468):1033-5.

30. Bird MI, Beaman RJ, Condie SA, Cooper A, Ulm S, Veth P. Palaeogeography and voyage modeling indicates early human colonization of Australia was likely from Timor-Roti. Quaternary Science Reviews. 2018;191:431-9.

31. Williams A, Ulm S, Turney C, Rohde D, White G. The establishment of complex society in prehistoric Australia: demographic and mobility changes in the Late Holocene. PLoS One. 2015;10(6):e0128661.

32. Moss PT, Dunbar GB, Thomas Z, Turney C, Kershaw AP, Jacobsen GE. A 60 000-year record of environmental change for the Wet Tropics of north-eastern Australia based on the ODP 820 marine core. Journal of Quaternary Science. 2017;32(6):704-16.

33. Tobler R, Rohrlach A, Soubrier J, Bover P, Llamas B, Tuke J, et al. Aboriginal mitogenomes reveal 50,000 years of regionalism in Australia. Nature. 2017;544:180.

34. Khan NS, Ashe E, Shaw TA, Vacchi M, Walker J, Peltier W, et al. Holocene relative sea-level changes from near-, intermediate-, and far-field locations. Current Climate Change Reports. 2015;1(4):247-62.

35. Murray-Wallace CV, Woodroffe CD. Quaternary sea-level changes: a global perspective: Cambridge University Press; 2014.

36. Williams AN, Ulm S, Sapienza T, Lewis S, Turney CSM. Sea-level change and demography during the last glacial termination and early Holocene across the Australian continent. Quaternary Science Reviews. 2018;182:144-54.

37. Sloss CR, Nothdurft L, Hua Q, O'Connor SG, Moss PT, Rosendahl D, et al. Holocene sea-level change and coastal landscape evolution in the southern Gulf of Carpentaria, Australia. The Holocene. in press;0(0):0959683618777070.

38. Lewis SE, Sloss CR, Murray-Wallace CV, Woodroffe CD, Smithers SG. Post-glacial sea-level changes around the Australian margin: A review. Quaternary Science Reviews. 2013;74:115-38.

39. Dougherty A, Dickson M. Sea level and storm control on the evolution of a chenier plain, Firth of Thames, New Zealand. Marine Geology. 2012;307:58-72.

40. Schellmann G, Radtke U. Timing and magnitude of Holocene sea-level changes along the middle and south Patagonian Atlantic coast derived from beach ridge systems, littoral terraces and valley-mouth terraces. Earth-Science Reviews. 2010;103(1-2):1-30.

41. Thom B, Chappell J. Holocene sea levels relative to Australia. Search. 1975;6(3):90-3.

42. Sloss CR, Murray-Wallace CV, Jones BG. Holocene sea-level change on the southeast coast of Australia: a review. The Holocene. 2007;17(7):999-1014.

43. Woodroffe SA. Testing models of mid to late Holocene sea-level change, North Queensland, Australia. Quaternary Science Reviews. 2009;28(23-24):2474-88.

44. Jones RS, Mackintosh AN, Norton KP, Golledge NR, Fogwill CJ, Kubik PW, et al. Rapid Holocene thinning of an East Antarctic outlet glacier driven by marine ice sheet instability. Nature Communications. 2015;6:8910.

45. Fogwill C, Turney C, Golledge N, Rood D, Hippe K, Wacker L, et al. Drivers of abrupt Holocene shifts in West Antarctic ice stream direction determined from combined ice sheet modelling and geologic signatures. Antarctic Science. 2014;26(6):674-86.

46. Rainsley E, Menviel L, Fogwill CJ, Turney CSM, Hughes ALC, Rood DH. Greenland ice mass loss during the Younger Dryas driven by Atlantic Meridional Overturning Circulation feedbacks. Scientific Reports. 2018;8(1):11307.

47. Fleming K, Lambeck K. Constraints on the Greenland Ice Sheet since the Last Glacial Maximum from sea-level observations and glacial-rebound models. Quaternary Science Reviews. 2004;23(9):1053-77.

48. Golledge NR, Thomas ZA, Levy RH, Gasson EG, Naish TR, McKay RM, et al. Antarctic climate and ice-sheet configuration during the early Pliocene interglacial at 4.23 Ma. Climate of the Past. 2017;13(7).

49. Lambeck K, Nakada M. Late Pleistocene and Holocene sea-level change along the Australian coast. Global and Planetary Change. 1990;3(1):143-76.

50. Thom B, Roy P. Sea level change in New South Wales over the past 15,000 years. Australian sea levels in the last. 1983;15(000):64-84.

51. Jones B, Youngt R, Eliot I. Stratigraphy and chronology of receding barrier-beach deposits on the northern Illawarra coast of New South Wales. Journal of the Geological Society of Australia. 1979;26(5-6):255-64.

52. Bryant EA, Young RW, Price DM, Short SA. Evidence for pleistocene and holocene raised marine deposits, Sandon Point, New South Wales. Australian Journal of Earth Sciences. 1992;39(4):481-93.

53. Short AD. Beaches of the New South Wales coast: a guide to their nature, characteristics, surf and safety: Sydney University Press; 2006.

54. Hogg AG, Hua Q, Blackwell PG, Niu M, Buck CE, Guilderson TP, et al. SHCal13 Southern Hemisphere calibration, 0–50,000 years cal BP. Radiocarbon. 2013;55(4):1889-903.

55. Dougherty AJ, Lynne BY, editors. Utilizing ground penetrating radar and infrared thermography to image vents and fractures in geothermal environments. Transactions - Geothermal Resources Council; 2011.

56. van Heteren S, Fitzgerald DM, Mckinlay PA, Buynevich IV. Radar facies of paraglacial barrier systems: coastal New England, USA. Sedimentology. 1998;45(1):181-200.

57. Turney CSM, Coope GR, Harkness DD, Lowe JJ, Walker MJC. Implications for the Dating of Wisconsinan (Weichselian) Late-Glacial Events of Systematic Radiocarbon Age Differences between Terrestrial Plant Macrofossils from a Site in SW Ireland. Quaternary Research. 2000;53(1):114-21.

58. Hogg AG, Fifield LK, Turney CSM, Palmer JG, Galbraith R, Baillie MGK. Dating ancient wood by high-sensitivity liquid scintillation counting and accelerator mass spectrometry—Pushing the boundaries. Quaternary Geochronology. 2006;1(4):241-8.

59. Bronk Ramsey C. Deposition models for chronological records. Quaternary Science Reviews. 2008;27(1-2):42-60.

60. Bronk Ramsey C, Lee S. Recent and planned developments of the program OxCal. Radiocarbon. 2013;55(2):720-30.

61. Bronk Ramsey C. Bayesian analysis of radiocarbon dates. Radiocarbon. 2009;51(1):337-60.

62. Van Loon AJ, Pisarska-Jamroży M. Chapter 4 - Changes in the Heavy-Mineral Spectra on Their Way From Various Sources to Joint Sinks: A Case Study of Pleistocene Sandurs and an Ice-Marginal Valley in Northwest Poland. In: Mazumder R, editor. Sediment Provenance: Elsevier; 2017. p. 49-62.

63. Hammer DA, Bastian R. Wetlands ecosystems: natural water purifiers. Constructed wetlands for wastewater treatment: municipal, industrial and agricultural. 1989;5.

64. Turney CSM, Roberts RG, de Jonge N, Prior C, Wilmshurst JM, McGlone MS, et al. Redating the advance of the New Zealand Franz Josef Glacier during the Last Termination: evidence for asynchronous climate change. Quaternary Science Reviews. 2007;26(25):3037-42.

65. McGlone MS, Wilmshurst JM. Dating initial Maori environmental impact in New Zealand. Quaternary International. 1999;59(1):5-16.

66. Colhoun E, editor Field problems of radiocarbon dating in Tasmania. Papers and proceedings of the Royal Society of Tasmania; 1986.

67. Roy P, Crawford E. Holocene geological evolution of the southern Botany Bay-Kurnell region, central New South Wales Coast: Department of Mineral Resources; 1976.

68. Reimer PJ, Bard E, Bayliss A, Beck JW, Blackwell PG, Ramsey CB, et al. IntCal13 and Marine13 radiocarbon age calibration curves 0–50,000 years cal BP. Radiocarbon. 2013;55(4):1869-87.

69. Ulm S. Australian marine reservoir effects: a guide toΔ R values. Australian Archaeology. 2006;63(1):57-60.

70. Fletcher M-S, Thomas I. A Holocene record of sea level, vegetation, people and fire from western Tasmania, Australia. The Holocene. 2010;20(3):351-61.

71. Martin ARH. Kurnell Fen: an eastern Australian coastal wetland, its Holocene vegetation, relevant to sea-level change and aboriginal land use. Review of Palaeobotany and Palynology. 1994;80(3):311-32.

72. Ramsey CB. Radiocarbon dating: revolutions in understanding. Archaeometry. 2008;50:249-75.

73. Bronk Ramsey C, Lee S. Recent and planned developments of the program OxCal. Radiocarbon. 2013;55(2-3):720-30.

Figure captions and Table:

Figure 1: Location of Bulli Beach (New South Wales, Australia) and key sites discussed in text. (a) Large scale regional map of Australia, (b) New South Wales coast with early Holocene Kurnell and Minnamurra sites shown in relation to Bulli. (c) 2013 air photograph of Bulli Beach and (d) overlay of a Digital Elevation Model (DEM) derived from LiDAR collected in 2013. Note, the yellow square and stars in panel c denote the benchmark and ^{14}C sampling sites north and south of Slacky Creek respectively. The DEM highlights the extent of the receded barrier (maroon and brown) backing the central portion of Bulli Beach and bisected by Slacky Creek. Also note the beach (green) and low-lying dune (yellow and orange) that has built since the 1974 storm, burying the peat surface.

Figure 2: Ground Penetrating Radar profile of Bulli Beach at Slacky Creek (NSW, Australia). (a) Oblique photograph looking south across Slacky Creek of peat exposed along Bulli beach after the 1974 storm (courtesy of Bob and Ann Young). (b) Northern GPR transect across present-day Bulli Beach imaging the buried peat surface with a strong reflection surface around an elevation of 1 m above MSL, similar to that found in the southern GPR transect (c). (d) The three-dimensional model used to image the peat surface in 3D (e). By isolating and interpolating between the high amplitude reflections caused by the peat surface, the lower amplitude signature within the overlying sand is stripped away, remotely sensing the lateral extent of the peat surface (e) previously exposed in 1974 (a).

Figure 3: Photographs of the Bulli mid-Holocene sea-level highstand level (taken shortly after the June 2016 storm). (a) Core location (white box) with limonite deposit marking the upper boundary of the estuarine sediments (white dashed lines). (b) Panorama of south-facing exposed estuarine sediment deposits (boundary with floodplain sediments marked by white dashed line) (c) North-facing view of the exposed estuarine sedimentary unit, with the dated wood (white box). Note, the keys used for scale in panels a and c).

Figure 4: Lithostratigraphy and OxCal age-depth model for the Bulli Beach (Slacky Creek South, NSW) using SHCal13 (54). The posterior and prior probability distributions are shown as dark and light respectively. The dark and light blue envelope provide the 1σ and 2σ calibrated age range respectively. Radiocarbon age laboratory numbers are denoted by the prefix 'Wk'. The anomalously older charcoal sample is shown in red.

Figure 5: Comparison between Bulli Beach (Slacky Creek; this study) and previously published Holocene sea level curve from the New South Wales coast (42). Anomalously older wood and charcoal samples are plotted for comparison. Timing of abrupt periods of Antarctic ice sheet surface lowering are shown for comparison (44, 45).

Table 1: Radiocarbon ages for Bulli and McCauley's beach estuarine sediments. The Bulli ages (obtained on the south side of Slacky Creek) have been modelled using the P_sequence and Outlier analysis option in OxCal 4.2 (72, 73) with SHCal13 (54). A_{model}=91.2; $A_{overall}$=83.

Profile and height above PSL, m	**Wk lab number**	**Material**	**^{14}C BP ± 1 σ**	**Modelled mean cal age (years, BP ± 1σ**
Slacky Creek (south)				
1.26	*43684*	Charcoal	6720±20	
1.19	*43685*	Plant fragments	6100±20	**6880±50**
0.40	*43686*	Plant fragments	6250±20	**7140±50**
0.31	*43687*	Plant fragments	6250±20	**7170±50**
0.04	*43688*	Plant fragments	6410±20	**7320±40**
-0.15	*43689*	Plant fragments	6610±20	**7450±30**
Slacky Creek (north)				
1.27	*43819*	Wood	6530±20	
1.27	*43820*	Wood	6380±20	
1.13	*43821*	Outer edge of *Melaleuca* log	6210±20	
1.13	*43822*	Contiguous (inner) sample of *Melaleuca* log	6300±20	
McCauley's Beach				
0.6	*43923*	Degraded wood	6820±20	
0.6	*43924*	Degraded wood	6610±20	

Figure

Click here to download Figure Fig_1.tif

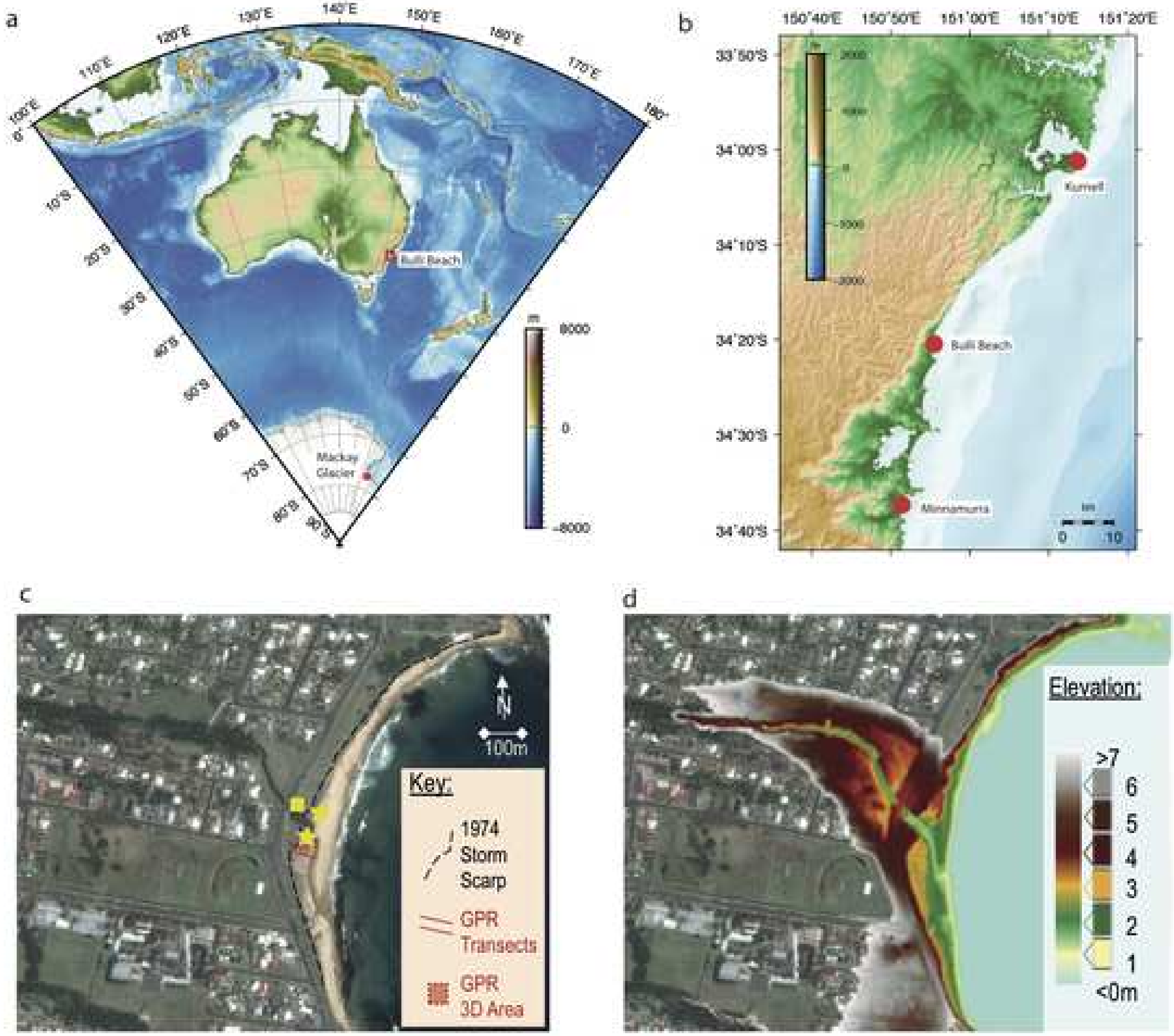

Figure

Click here to download Figure Fig_2.tif

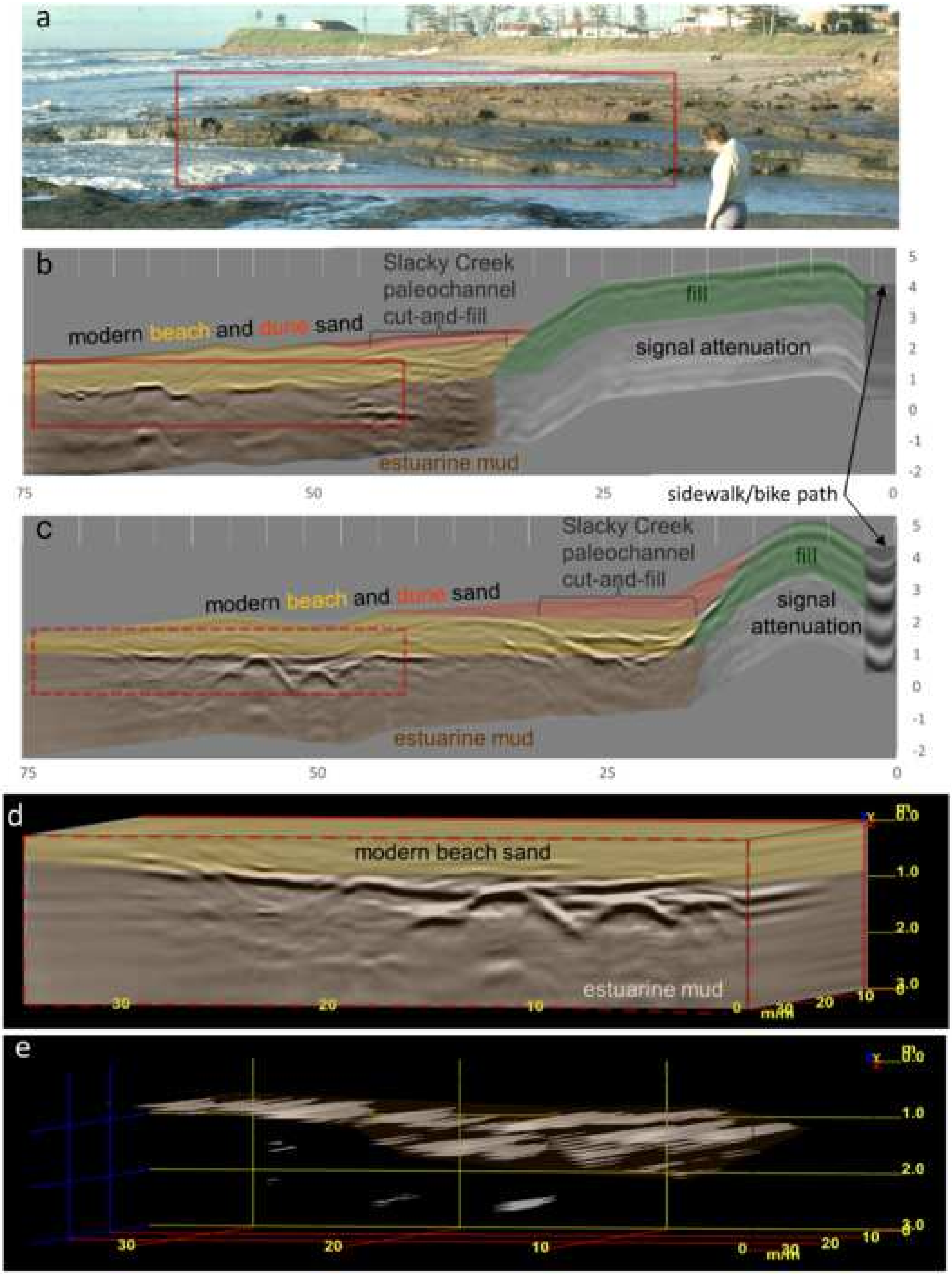

Figure 2

Figure

Click here to download Figure Fig_3.tif

Figure

Click here to download Figure Fig_4.tif

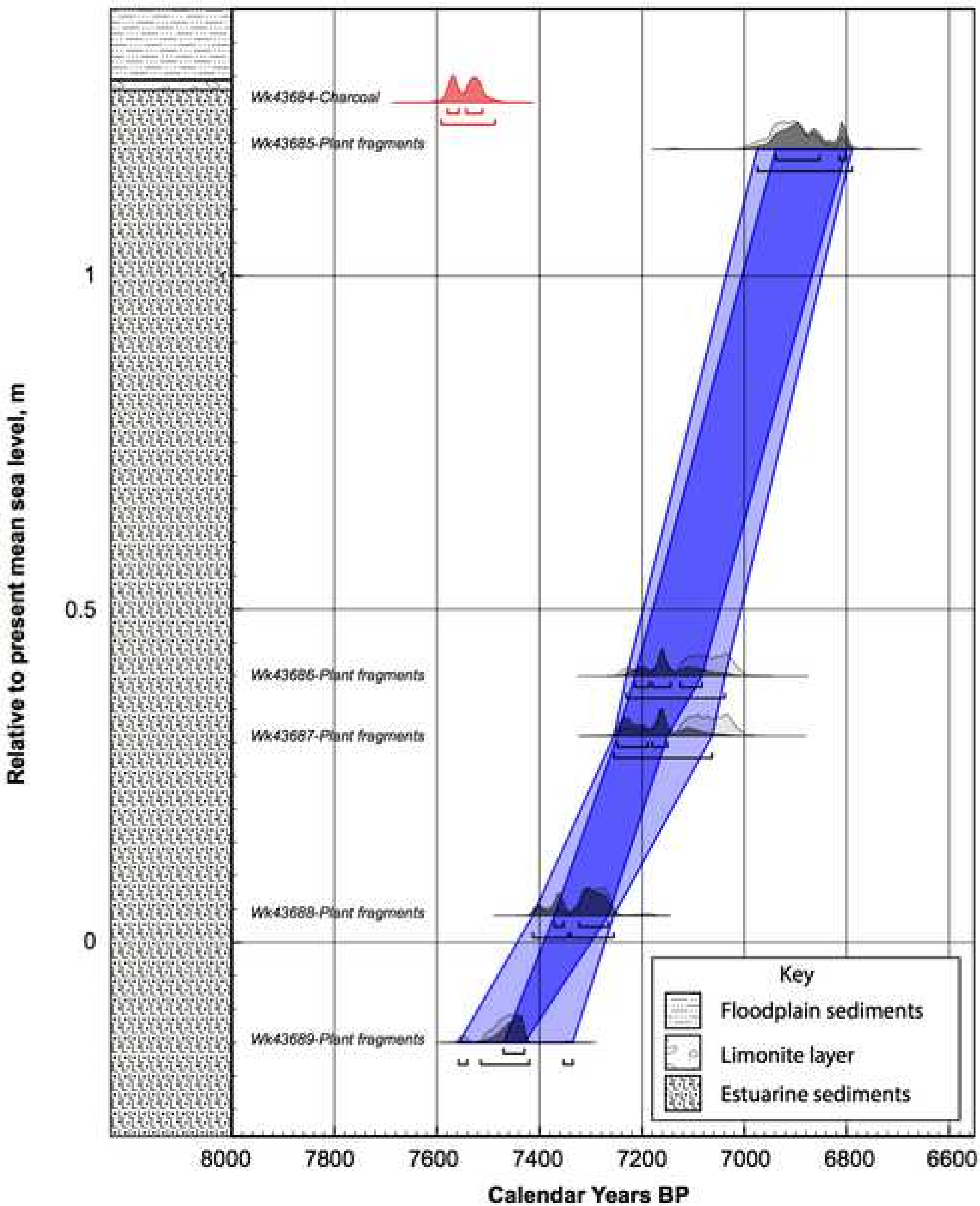

Figure

Click here to download Figure Fig_5.tif